Synthesis and structures of the dinuclear tin(II) complexes [Sn{μ-C(R)X(Z)NSiMe₃}]₂ [R = Ph, X(Z) = CPh; R = SiMe₃, X(Z) = PPh₂] and of related compounds

Peter B. Hitchcock [a], Michael F. Lappert [a,*], Mikko Linnolahti [b], John R. Severn [a], Patrick G.H. Uiterweerd [a], Zhong-Xia Wang [a,1]

[a] Department of Chemistry, University of Sussex, Brighton BN1 9QJ, UK
[b] Department of Chemistry, University of Joensuu, P.O. Box 111, 810101 Joensuu, Finland

ARTICLE INFO

ABSTRACT

Tin(II) compounds containing the ligands [CH(C₆H₃Me₂-2,5)C(Buᵗ)NSiMe₃]⁻ (≡ L^1), [CH(Ph)C(Ph)NSiMe₃]⁻ (≡ L^2), [CH(SiMe₃)P(Ph)₂NSiMe₃]⁻ (≡ L^3), [CH(SiMe₃)P̄(Ph)=NSi(Me)₂C₆H₄-1,2]⁻ (≡ L^4), [C(Ph)C(Ph)-NSiMe₃]²⁻ (≡ L^5), and [C(SiMe₃)P(Ph)₂NSiMe₃]²⁻ (≡ L^6) are reported: the transient SnBr(L^1) (1) and SnBr(L^2) (2), Sn(L^1)₂ (3) [P.B. Hitchcock, J. Hu, M.F. Lappert, M. Layh, J.R. Severn, J. Chem. Soc., Chem. Commun. (1997) 1189], the labile Sn(L^2)₂ (4), [Sn(L^5)]₂ (5), SnCl(L^3) (6), Sn(L^3)₂ (7), [Sn(L^6)]₂ (8), Sn(L^4)₂ (9) and Pb(L^4)₂ (10). They were prepared from (i) SnBr₂ and K(L^1) (1, 3) or K(L^2) (2, 4, 5); (ii) SnCl₂ and Li(L^3) (6–9); or (iii) PbCl₂ and Li(L^4) (10). Each of 1, 3 and 5–10 has been characterised by multinuclear NMR spectra; 3, 5, 6, 8, 9 and 10 by EI-mass spectra, but only 3, 5, 8, 9 and 10 were isolated pure and furnished X-ray quality crystals. Of greatest novelty are the title binuclear fused tricyclic ladder-like compounds 5 and 8. Quantum chemical calculations, on alternative pathways to 5 from 2 and to 8 from 7, are reported.

© 2009 Elsevier B.V. All rights reserved.

1. Introduction

Until the early 1970's, most of the published work on the metallic elements of Group 14 (Ge, Sn, Pb) concentrated exclusively on the tetravalent state. Relatively few divalent germanium, tin or lead compounds had been fully characterised due to their low stability or to their strong tendency towards polymerisation [1–4]. Over the next 10–15 years this previously neglected area of chemistry grew enormously as the crucial role of ligand design in the kinetic stabilization of compounds through steric effects was recognised. The use of various sterically demanding ligands gave thermally stable Ge(II), Sn(II) or Pb(II) monomers or dimers; a series of such ligands was developed, which included amido, alkoxo, aryloxo, alkylthio, alkyl, aryl and cyclopentadienyl ligands [3–6]. Monoanionic N-centred chelating ligands which have featured in group 14 metal(II) chemistry include β-diiminates [7]. More directly relevant to the present paper are tin(II) compounds containing monoanionic, usually chelating, 1,3-N,X-centred ligands: (i) X = N, the amidinates [8,9] and guanidinates [9] and quite specifically (ii) (X = C) the 1-azaallyls [10]. 1-Iminodiarylphosphoranylmethyls and some of their tin(II) derivatives, which like (ii) are the focus of the present report, were previously unknown, but related compounds are A [11], B [12a] and C [12b]. Earlier publications [related to (ii)] dealt with the synthesis and structures of the compounds D [13], E [14], F [14], G [15], and H [15,16]; the structure of crystalline 3 (vide infra) has also been published [15].

The present paper is a contribution to our pioneering studies on novel divalent molecular compounds of tin. Four of the ligands chosen (L^1–L^4) are 1,3-N,C-centred and potentially chelating, characterised by having a potentially labile hydrogen attached to the 3-carbon atom; two of these (L^2 and L^4) are unprecedented and another two (L^1 and L^3) have appeared only briefly in our prior publications.

* Corresponding author. Tel.: +44 1273 678316; fax: +44 1273 876687.
E-mail address: m.f.lappert@sussex.ac.uk (M.F. Lappert).
1 Present address: Department of Chemistry, University of Science and Technology of China, Hefei, Anhui 230026, PR China.

$$[\overline{Sn\{N(SiMe_3)C(Bu^t)}C(H)SiMe_3\}_2]$$

G

$$[Sn\{N(SiMe_3)C(Ph)C(SiMe_3)_2\}\{N(SiMe_3)C(Ph)=C(SiMe_3)_2\}]$$

H
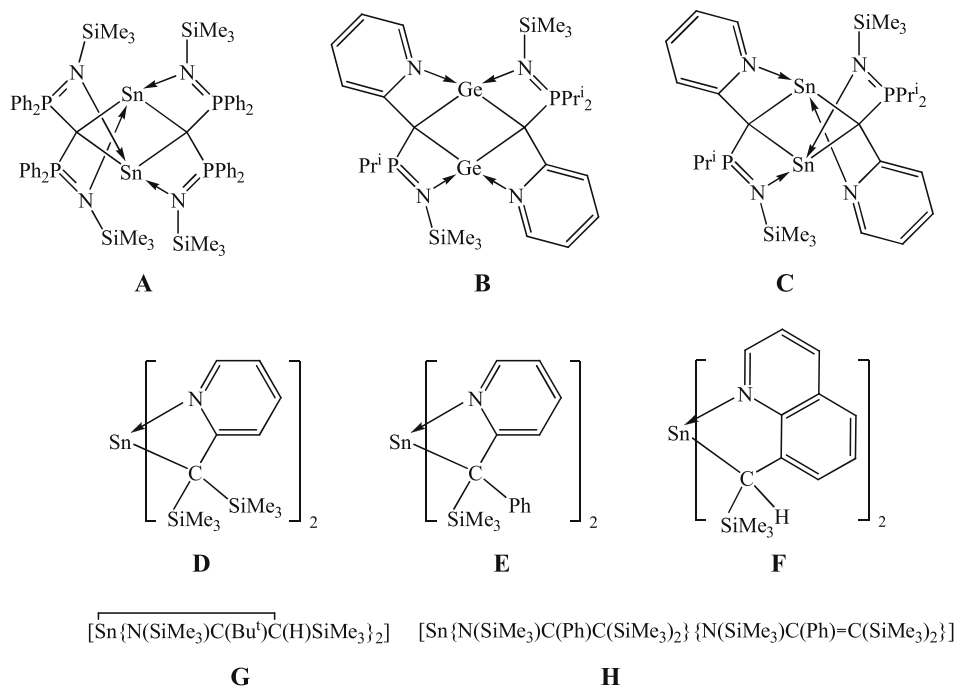
2. Results and discussion

This paper deals with the synthesis and structures of tin(II) compounds containing the ligands $\mathbf{L^1}$–$\mathbf{L^6}$. Each is an 1,3-C,N-chelating moiety having an NZC core; four are monoanionic having Z = CR′ ($\mathbf{L^1}$, $\mathbf{L^2}$) or PPh(C₆H₄R″-2) ($\mathbf{L^3}$, $\mathbf{L^4}$), and two are dianionic with Z = CPh ($\mathbf{L^5}$) or PPh₂ ($\mathbf{L^6}$).

itant 1,3-C → N shift of the SiMe₃ group, is a variant of a general route described earlier [17]. Both the prior ambient temperature lithiation of the SiMe₃- and aryl-activated methane, and the ultimate conversion of the hydrocarbon-soluble Li($\mathbf{L^1}$ or $\mathbf{L^2}$) into the insoluble K($\mathbf{L^1}$ or $\mathbf{L^2}$), have ample precedent [18].

$\mathbf{L^1}$: R¹ = Buᵗ, R² = C₆H₃Me₂-2,5
$\mathbf{L^2}$: R¹ = Ph = R²
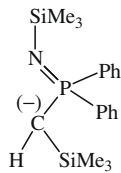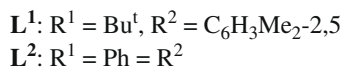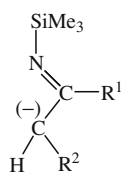
$\mathbf{L^3}$
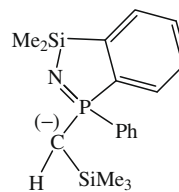
$\mathbf{L^4}$
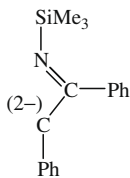
$\mathbf{L^5}$
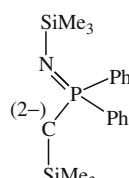
$\mathbf{L^6}$

2.1. The tin(II) compounds 1–5

The 1-azaallylpotassium compounds K($\mathbf{L^1}$) and K($\mathbf{L^2}$) were prepared in high yield, as shown in Schemes 1 and 2. The procedure, in which the key step was the insertion of the α-hydrogen-free nitrile (BuᵗCN or PhCN) into the appropriate lithium trimethylsilylalkyl [LiCH(SiMe₃)(C₆H₃Me₂-2,5) for Li($\mathbf{L^1}$) or LiCH-(SiMe₃)Ph for Li($\mathbf{L^2}$), respectively] with concom-

The reaction of tin(II) bromide with two equivalents of K($\mathbf{L^1}$) or K($\mathbf{L^2}$) gave the yellow crystalline complexes Sn($\mathbf{L^1}$)₂ (**3**) or [Sn($\mathbf{L^5}$)]₂ (**5**), respectively. It is suggested (Scheme 3) that the formation of each proceeded via the intermediate Sn(Br)$\mathbf{L^1}$ (**1**) or SnBr($\mathbf{L^2}$) (**2**), respectively, the latter furnishing first the labile Sn($\mathbf{L^2}$)₂ (**4**) which, being sterically encumbered, eliminated H($\mathbf{L^2}$) en route to **5**. The structure (but no other data) for crystalline **3** has previously been communicated [15]; and selected geometrical parameters are shown in Fig. 1.

$$2,5\text{-}Me_2C_6H_3CH_2Cl \xrightarrow[\text{2. Si(Cl)Me}_3]{\text{1. Mg, Et}_2O} 2,5\text{-}Me_2C_6H_3CH_2SiMe_3 \xrightarrow[\text{2. Bu}^t\text{CN, KOBu}^t]{\text{1. LiBu}^n,\text{ tmeda, C}_5H_{12}}$$

$$K[CH(C_6H_3Me_2\text{-}2,5)C(Bu^t)NSiMe_3]$$

$$[\equiv K(\mathbf{L}^1)],\ 94\%$$

Scheme 1.

$$PhCH_2SiMe_3 \xrightarrow{\text{LiBu}^n,\text{ tmeda, C}_5H_{12}} Li[CH(SiMe_3)Ph] \xrightarrow[\text{2. KOBu}^t]{\text{1. PhCN, C}_5H_{12}} K[CH(Ph)C(Ph)NSiMe_3]$$

$$[\equiv K(\mathbf{L}^2)],\ 74\%$$
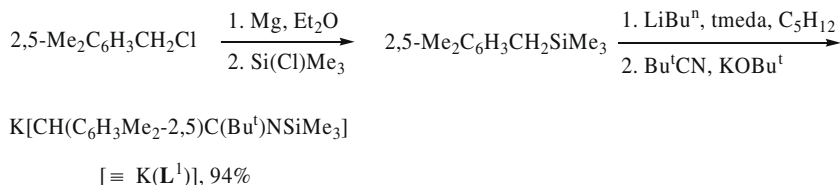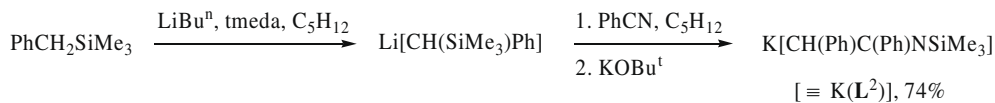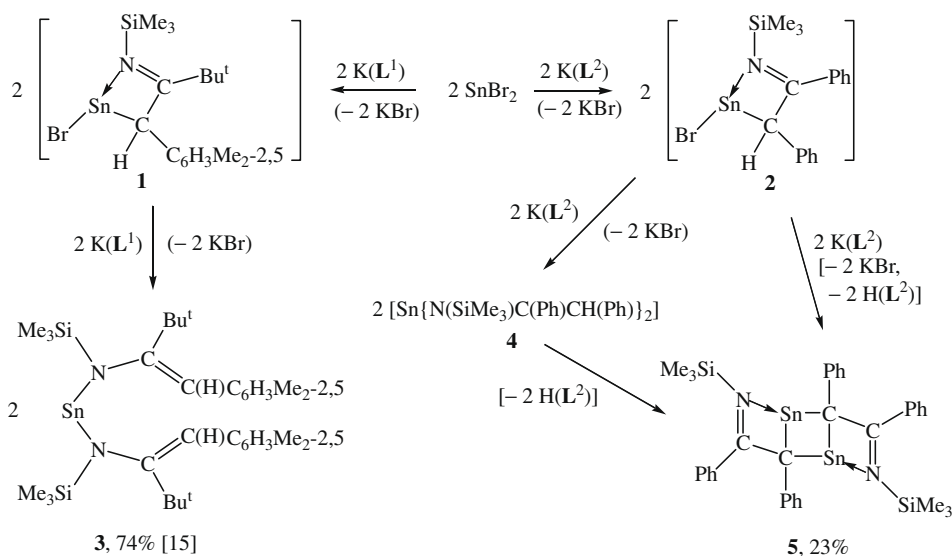
Scheme 2.

Scheme 3.
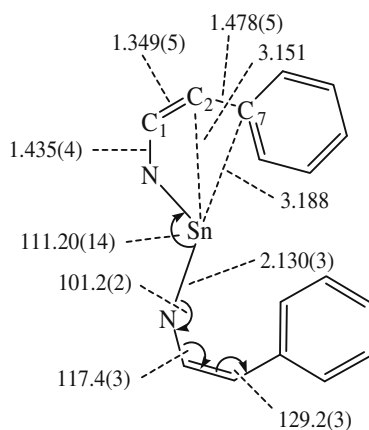
Fig. 1. Selected structural parameters of crystalline Sn($\mathbf{L}^1$)$_2$ (**3**); core atoms only [15].
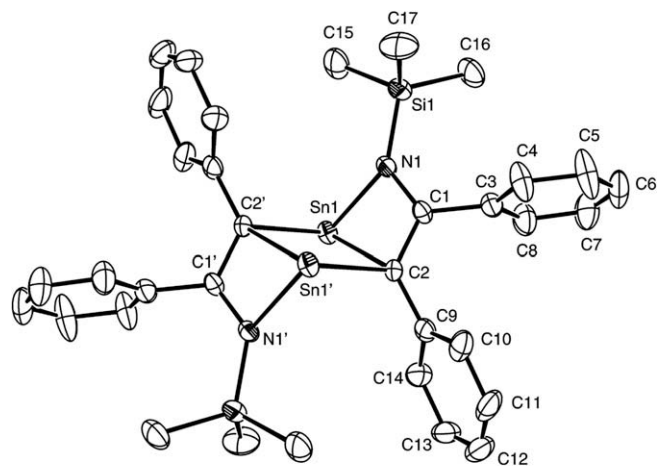
Fig. 2. Molecular structure of [Sn($\mathbf{L}^5$)]$_2$ (**5**) in ORTEP representation.

Compounds **3** and **5** gave satisfactory C, H and N microanalyses. The EI-mass spectra showed parent molecular cations for the mononuclear **3** and the dinuclear **5** and appropriate fragment ions. The multinuclear NMR spectra for **3** in C$_6$D$_6$ at ambient temperature were consistent with the crystal structure; the ^{119}Sn{^{1}H}

NMR chemical shift of δ +61.5 ppm may be compared with the δ −387.2 and δ −37.3 ppm for **G** and **H**, respectively [15], and the δ +148.4 (323 K) and +118.5 (213 K) for **A** [13].

Compound **5** was too sparingly soluble in hydrocarbon solvents to locate ^{1}H NMR spectral signals. However, solution ^{1}H NMR data,

Table 1
Selected bond distances (Å) and angles (°) for **5**.

Sn1–N1	2.216(5)	N1–Si1	1.742(6)
Sn1–C2	2.317(6)	C1–C3	1.513(9)
Sn1–C2′	2.318(7)	C2–C9	1.466(9)
N1–C1	1.334(8)	Sn1···Sn1′	3.132(2)
C1–C2	1.406(9)		
N1–Sn1–C2	61.7(2)	Sn1–C2–C1	84.4(4)
C2–Sn1–C2′	95.0(2)	Sn1–C2–Sn1′	85.0(2)
N1–C1–C2	116.1(6)	Sn1–N1–Si1	133.7(3)
N1–C1–C3	121.7(6)	C1–C2–C9	126.1(6)
N1–Sn1–C2′	97.5(2)	C1–N1–Sn1	90.2(4)

Symmetry transformations to generate equivalent atoms ′−x + 1, −y + 1, −z + 1. ″−x + 1, −y, −z + 1.

clearly of a diamagnetic material, were collected in C_5D_5N at ambient temperature; the signals, characteristic of the L^2 ligand, were of low intensity and consequently attempts to obtain spectral data for other nuclei were unsuccessful. In the light of the microanalytical, mass spectral and particularly the X-ray data (see next paragraph) on crystalline **5**, this NMR spectrum is attributed to **4** or $H(L^2)$ rather than **5**.

The molecular structure of the crystalline, centro-symmetric fused tricyclic ladder compound $[Sn(L^5)]_2$ (**5**) is shown in an ORTEP representation in Fig. 2. Selected bond lengths and angles are listed in Table 1. The central rhomboidal Sn1C2Sn1′C2′ ring has the endocyclic angles subtended at the tin atoms ca. 10° wider than those at carbon. The transannular Sn···Sn′ distance is too long for there to be significant bonding between them; tin–tin single bonds are generally in the range 2.75–2.92 Å [19]. The outer Sn1N1C1C2 and Sn1′N1′C1′C2′ rings are puckered, the dihedral angle between the Sn1N1C1 and Sn1C2C1 planes is 27.4° and that between the latter and the Sn1C2Sn1′ is 68.6°. Comparisons with the structure of **8** are deferred to Section 2.2.

To investigate possible reaction pathways further, quantum chemical calculations studies were performed. Scheme 4 illustrates the first pathway to **5** via **4** in more detail, and includes the possi-

ble structures of isomers **4a**–**4c** of the latter and of the by-product $H(L^2)$ as monomer or dimer. The calculations were carried out using two methods: initially by the hybrid density functional B3LYP/def2-SVP procedure, involving the screening of isomeric possibilities. The final calculations, on the energetically preferred isomers, were performed at the MP2/def-TZVP level. The use of MP2 was necessary mainly because of dispersive interactions between the phenyl groups, which is one of the most well-known problems of density functional theory. Also the possibility for the side-product to form a hydrogen-bonded dimer was an issue.

Concerning the isomeric forms of **4**, there are many possibilities for the rings to arrange around the tin centre. Having calculated 12 different isomers (at B3LYP level), the energetically preferred are illustrated in Fig. 3, with their energies and selected calculated bond lengths and angles (MP2). As evident from Fig. 3, **4c** lies 33.1 kJ/mol higher in energy than **4a**; attempts to locate **4b** resulted in a transformation back to **4a**.

Four separate isomers of the monomeric side-product (HL^2) were calculated; the energetically preferred is illustrated in Fig. 4, showing the relative arrangement of its two phenyl groups and the localisation of the hydrogen atom attached to the nitrogen. For the dimeric side-product, only one possibility was considered as no reasonable alternative was envisaged. In the dimer the arrangement of the phenyl groups is different and the hydrogen atoms of $(HL^2)_2$ are located on carbon rather than nitrogen. The Gibbs free energies as a function of temperature (illustrated in the Supplementary data) for the dimerisation of HL^2, showed that HL^2 exists as a dimer at temperature ⩽ 210 K.

Fig. 5 shows the computed molecular structure of $[Sn(L^5)]_2$ (**5**) with selected calculated and observed geometrical parameters.

The Gibbs free energy for the conversion of **4a** into **5**, with monomeric and dimeric HL^2 as co-products calculated over a range of temperatures is illustrated in the Supplementary data. It is concluded that these reactions are exothermic above 200 K.

Quantum chemical calculation studies were also carried out on the alternative pathway to **5**, from **2** without the intermediate of **4**,


Scheme 4.

4a
($\Delta E = 0.0$ kJ/mol).
C_2-symmetry
Sn–N: 2.166 Å
Sn–C (CH): 2.832 Å
N–Sn–N: 100.1°

4c
($\Delta E = 33.1$ kJ/mol).
C_2-symmetry
Sn–N: 2.447 Å
Sn–C: 2.383 Å
N–Sn–N: 143.0°
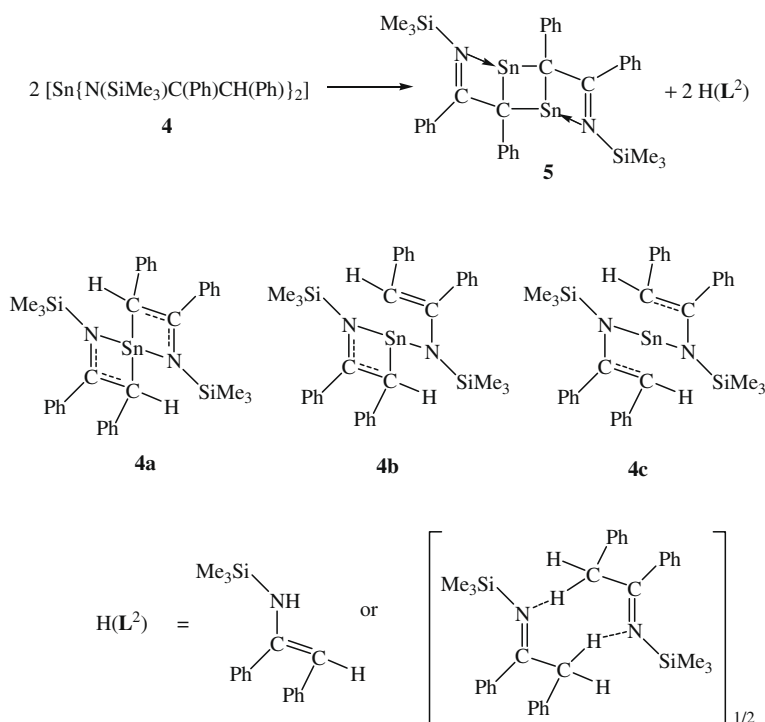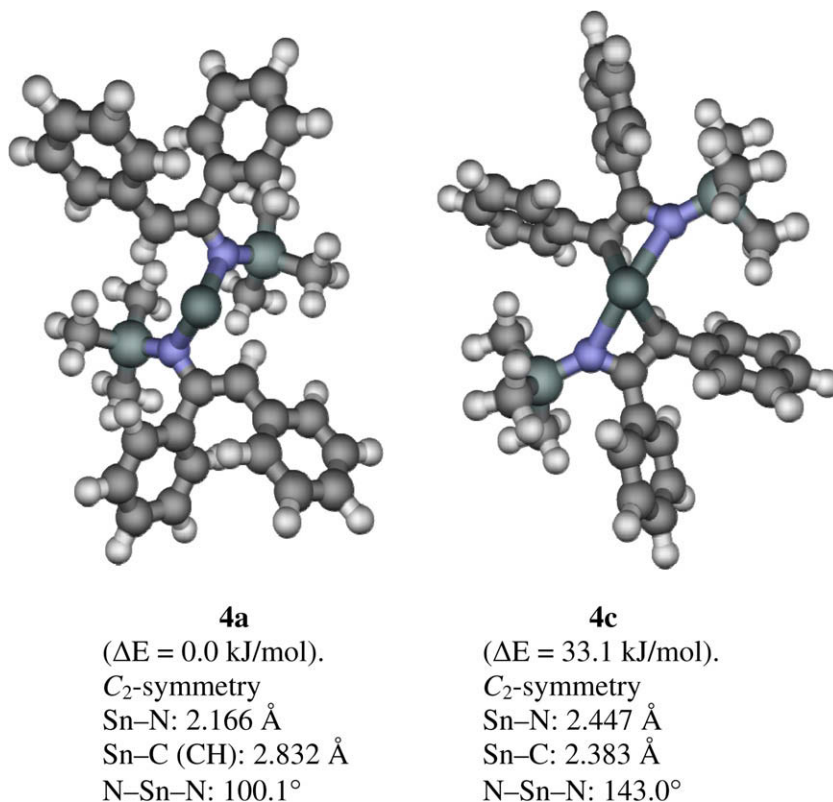
Fig. 3. MP2 calculated structure for isomer **4a** and **4c**, with selected bond angles and lengths.


HL^2 $[HL^2]_2$
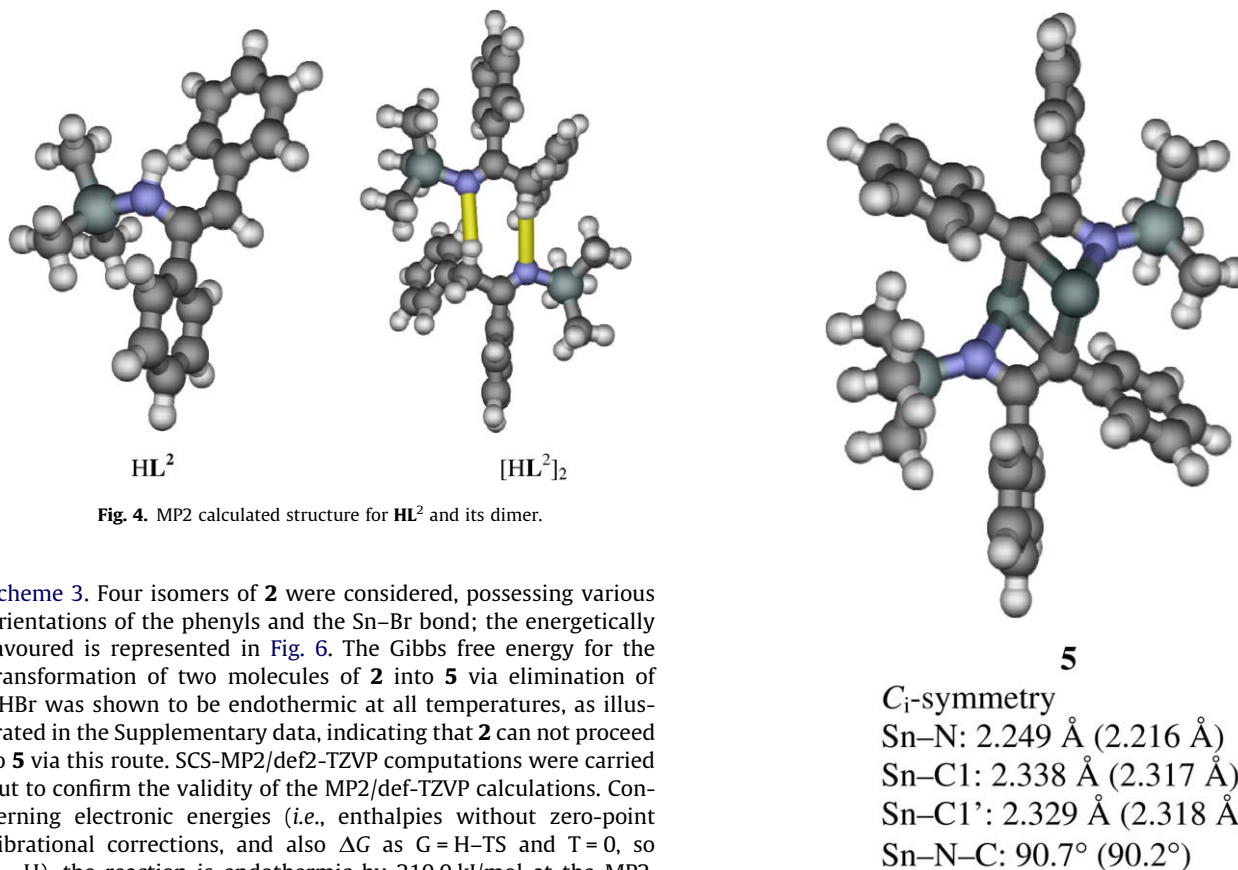
Fig. 4. MP2 calculated structure for HL^2 and its dimer.

Scheme 3. Four isomers of **2** were considered, possessing various orientations of the phenyls and the Sn–Br bond; the energetically favoured is represented in Fig. 6. The Gibbs free energy for the transformation of two molecules of **2** into **5** via elimination of 2HBr was shown to be endothermic at all temperatures, as illustrated in the Supplementary data, indicating that **2** can not proceed to **5** via this route. SCS-MP2/def2-TZVP computations were carried out to confirm the validity of the MP2/def-TZVP calculations. Concerning electronic energies (*i.e.*, enthalpies without zero-point vibrational corrections, and also ΔG as G = H–TS and T = 0, so G = H), the reaction is endothermic by 210.0 kJ/mol at the MP2, and even more so at the SCS-MP2 level, 222.7 kJ/mol (B3LYP gives the even much higher value of 342.2 kJ/mol).

5
C_i-symmetry
Sn–N: 2.249 Å (2.216 Å)
Sn–C1: 2.338 Å (2.317 Å)
Sn–C1': 2.329 Å (2.318 Å)
Sn–N–C: 90.7° (90.2°)

Fig. 5. MP2 computed structure for **5**, with selected calculated bond lengths and an angle with crystal structural data in parentheses.
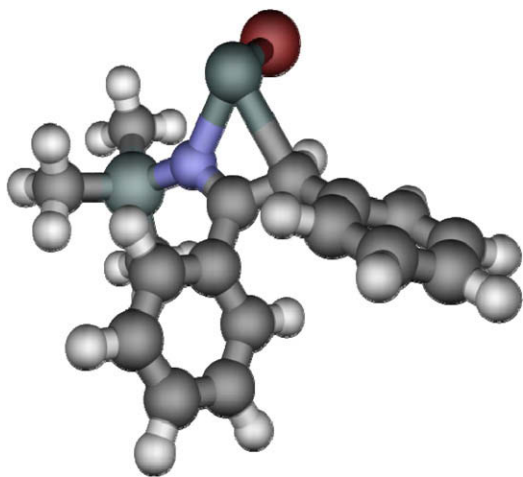
2

C_1-symmetry
Sn–N: 2.195 Å
Sn–C: 2.541 Å
Sn–Br: 2.616 Å
Br–H: 3.060 Å

Fig. 6. MP2 calculated structure for **2**.

2.2. The tin(II) compounds **6–9** and the lead(II) compound **10**

The synthesis of the new crystalline tin(II) complexes, the yellow binuclear [Sn(L^6)]$_2$ (**8**) and the colourless mononuclear Sn(L^4)$_2$ (**9**), is outlined in Scheme 5. The precursors were SnCl$_2$ and the 1,3-bis(trimethylsilyl)-1-aza-2-diphenylphospha(V)allyllithium compound Li(L^3). An *in situ*-prepared Li(L^3) had been used for the synthesis of the X-ray-characterised Pb(L^3)$_2$ (Fig. 7) [20]; the synthesis and X-ray structures of the crystalline complexes Li(L^3)(OEt$_2$) and [Li(L^3)]$_2$ have been reported [21]. Treatment of SnCl$_2$ with two equivalents of an *in situ*-prepared portion of Li(L^3) in Et$_2$O at −40 °C, removal of volatiles and extraction of the residue with pentane afforded a high yield (based on SnCl$_2$) of yellow crystals of **8**. At ambient temperature **8** proved to be thermally

labile, the solid being stable only for *ca.* 3 weeks and a C$_6$D$_6$ solution only for *ca.* 4 d; whilst at −30 °C it suffered no deterioration, either as solid or in hydrocarbon solution, after being stored at that temperature for three months.

Surprisingly, from equivalent portions of SnCl$_2$ and Li(L^3) in Et$_2$O, then addition of an equivalent portion of LiBu^n in hexane, followed by removal of solvent *in vacuo*, extraction of the residue with hexane and concentration of the extract furnished colourless crystals of Sn(L^4)$_2$ (**9**) in 54% yield [based on Li(L^3)].

Evidence for SnCl(L^3) (**6**) as an intermediate in these reactions was realised by mass spectral data on the material obtained by the following procedure. Equivalent portions of SnCl$_2$ and Li(L^3) in Et$_2$O were allowed to react for 15 h at ambient temperature, then filtered, the filtrate was concentrated and hexane added yielding a white solid, which contained **6** as judged by its EI-mass spectrum, and its ^{1}H NMR spectrum in C$_6$D$_6$.

Whereas 2 Li(L^3) + PbCl$_2$ at −45–0 °C in Et$_2$O gave the X-ray-characterised Pb(L^3)$_2$ [20], the same reagents under prolonged reflux furnished Pb(L^4)$_2$ (**10**), Eq. (1). It is likely that Pb(L^3)$_2$ was an intermediate along the pathway to Pb(L^4)$_2$. The tin analogue **7** of the latter, although not isolated pure, was obtained contaminated with H(L^3) as the first formed product en route to [Sn(L^6)]$_2$ (**8**). Thus, the ^{1}H NMR spectrum of freshly prepared **7** invariably showed the presence of H(L^3), doublets being observed at δ 1.44 [H(L^3)] and 1.71 (**7**) ppm. The production of H(L^3) was not a result of purification difficulties, because upon heating the CH signal at δ 1.71 ppm disappeared whilst that at δ 1.44 ppm increased in intensity; furthermore, the ^{1}H{^{31}P} NMR spectrum showed singlet signals for the CH protons. A freshly prepared sample of **7** [with H(L^3)] revealed the expected triplet, due to $^2J(^{119}$Sn–^{31}P), in the ^{119}Sn{^{1}H} NMR spectrum at δ 82.3 ppm which upon heating disappeared and concomitantly a new triplet signal at δ 530.3 (attributed to **8**) was observed. Similar features were found in the ^{31}P{^{1}H} NMR spectra: thus, initially the main *P*-containing constituent was **7** [δ 25.45 ppm], but upon heating this signal vanished, whilst that at δ 0.46 ppm of H(L^3) progressively increased in intensity as did a new signal at δ 27.77 ppm (due to **8**). Based on $\delta(^{207}$Pb) for Pb(L^3)$_2$ of 2788 ppm [20], the calculated value of $\delta(^{119}$Sn) for Sn(L^3)$_2$ (**7**) is 137 ppm based on the empirical correlation of Eq. (2) (ref. [22]) [22], which, whilst not very close to the assigned chemical shift of δ 82.3 ppm, is of a similar order of magnitude keeping in mind the very wide range of known ^{119}Sn chemical shifts. Selected NMR data for **7** and **8** are compared with those for four related compounds in Table 2.
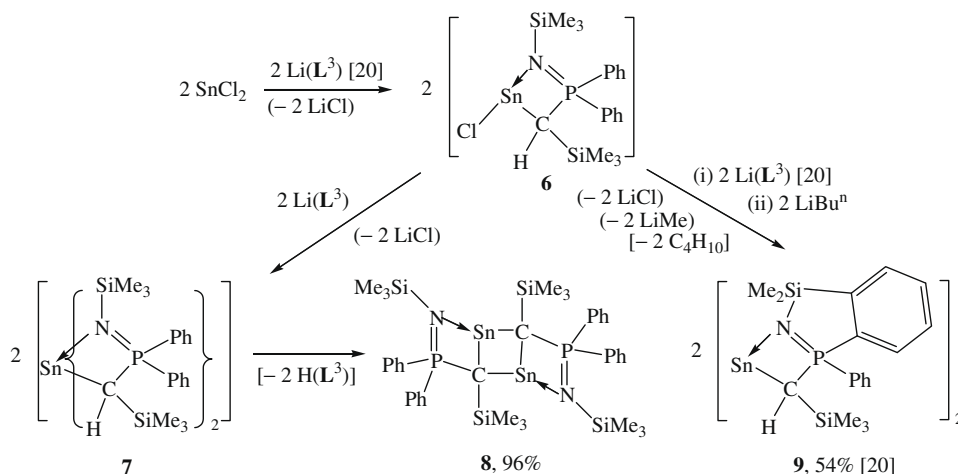

Scheme 5.
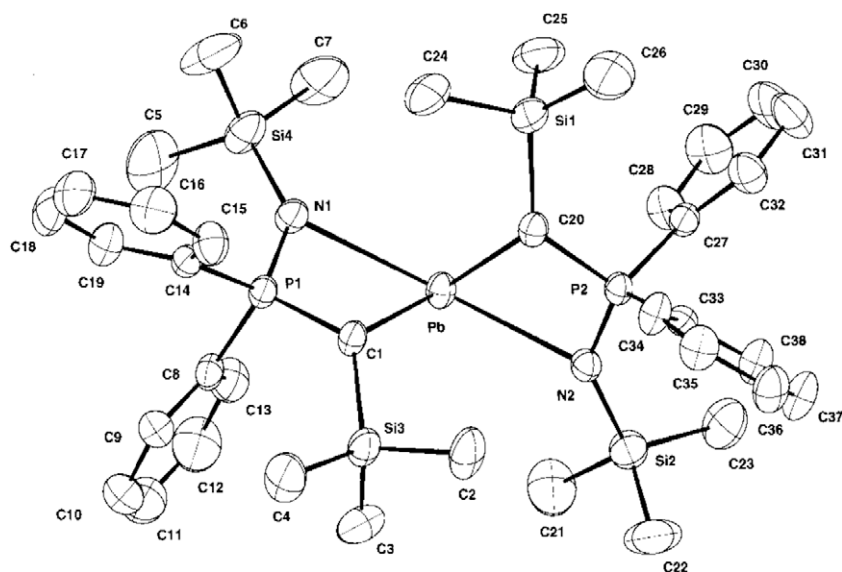
Fig. 7. Selected structural parameters of crystalline Pb(L³)₂: Pb–N1 2.701(4), Pb–N2 2.654(4), Pb–C1 2.449(6), Pb–C20 2.447(5) Å; N1–Pb–C1 62.52(14), N1–Pb–N2 162.27(1), N1–Pb–C20 107.6(2), N2–Pb–C1 106.49(14), C1–Pb–C20 88.2(2)° [20].

Table 2
Selected solution NMR spectroscopic data in C_6D_6 or C_7D_8 for **7** and **8** and four reference compounds at ambient temperature.

Compound	H(L3)[a]	[Li(L³)(OEt₂)][b]	[Li(L³)]₂[b]	Sn(L³)₂ (**7**)	Pb(L³)₂[c]	[Sn(L⁶)]₂ (**8**)
δ (C¹H)/ppm	1.44 (d)	1.48 (d)	1.47 (d)	1.71 (d)	1.37 (d)	–
²J(¹H–³¹P)/Hz	15.2	14.7	13.8	15.7	15.8	–
δ [³¹P{¹H}]/ppm	0.46	60.0	33.32	25.45	19.52	27.77
δ [¹¹⁹Sn{¹H}]/ppm	–	–	–	82.3 (t)	–	530.3 (t)

[a] Ref. [23].
[b] Ref. [21].
[c] Ref. [20].

$$PbCl_2 + 2Li(\mathbf{L^4}) \xrightarrow{\text{Et}_2\text{O}} 2LiCl + \underset{\mathbf{10},48\%}{Pb(\mathbf{L^4})_2} \qquad (1)$$
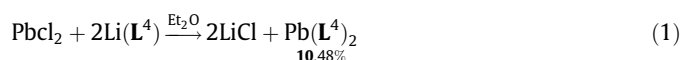
$$\delta(^{207}Pb) = 3.30[\delta(^{119}Sn)] + 2336 \qquad (2)\,(\text{ref.}[22])$$

Satisfactory C, H, N microanalytical data were obtained for [Sn(L⁶)]₂ (**8**), Sn(L⁴)₂ (**9**) and Pb(L⁴)₂ (**10**). The δ(³¹P) and δ(¹¹⁹Sn) NMR chemical shifts for **8** are listed in Table 2.
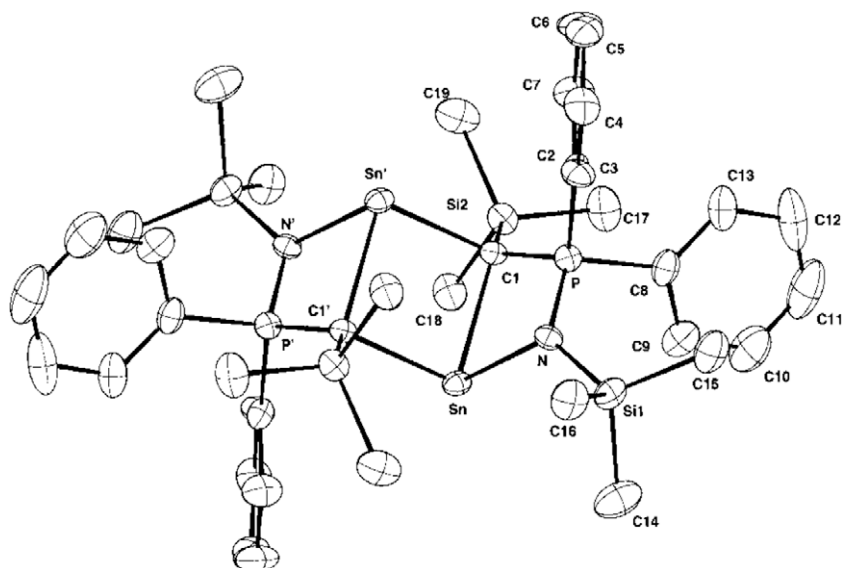

Fig. 8. Selected structural parameters of crystalline [Sn(L⁶)]₂ (**8**) (see also Fig. 12): C1–P 1.706(8), Sn–N 2.308(7), P–N 1.618(7) Å; Sn′–C1–P 110.5(4), C1–P–N 105.0(4), C1–Sn′–N′ 99.0(3), Sn–C1′–P′ 110.5(4), P–N–Sn 92.6(3)° [24].

I [25]

5 (*a*)   (*b*)   (*c*)
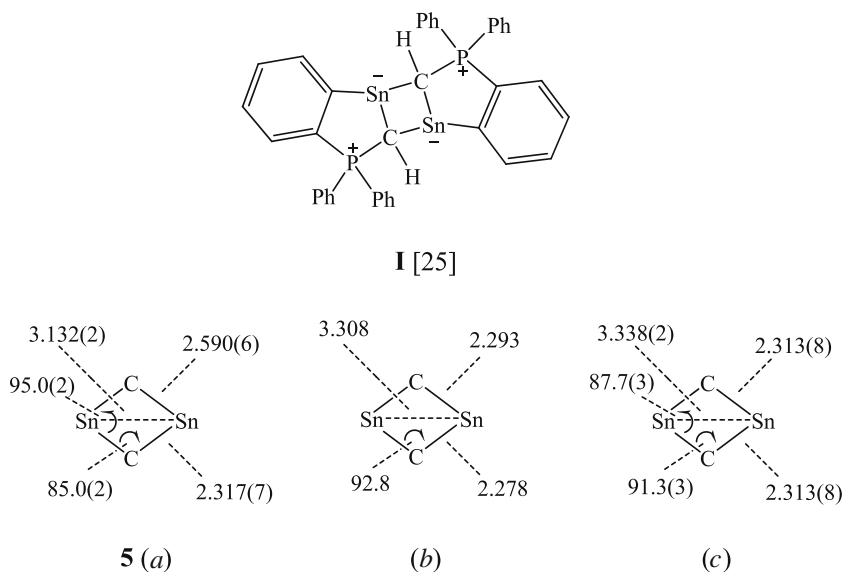
Fig. 9. Comparative geometric data for the SnC1Sn′C1′ fragment of **5** (*a*), **I** (*b*) [25] and **8** (*c*).

The ^{1}H NMR spectral data for **9** in C_6D_6 at ambient temperature includes a singlet (SiMe$_3$) and a doublet (SiMe$_2$); the latter is attributed to the *exo*- and *endo*-methyls of the CCPNSi ring. Likewise, the ^{13}C{^{1}H} NMR spectrum showed three sets of silylmethyl signals, each a doublet due to J([13]C–[31]P). The ^{119}Sn{^{1}H} NMR spectrum revealed a triplet due to coupling to two equivalent ^{31}P nuclei, whilst the ^{31}P{^{1}H} NMR spectrum had [119/117]Sn satellites. The ^{29}Si{^{1}H} NMR spectrum contained a singlet with [119/117]Sn satellites and a doublet due to coupling to [31]P.

The ^{1}H and ^{13}C{^{1}H} NMR spectra of **10** in C_6D_6 showed three sets of silylmethyl signals assigned (as for **9**) to SiMe$_3$ and *exo*-/*endo*-SiMe$_2$ methyls. The [31]P{^{1}H} and the [207]Pb{^{1}H} NMR spectra revealed a singlet with [207]Pb satellites and a triplet due to ^{31}P-coupling, respectively.

The molecular structure of the centro-symmetric crystalline **8** is shown in Fig. 8, with selected geometrical parameters. It has a fused tricyclic ladder-like skeleton. The central SnC1Sn′C1′ ring is planar and its geometric parameters are similar to those for the corresponding in [Sn(L^6)]$_2$ (**5**) and Veith and Huch's compound **I** [25], as illustrated in Fig. 9. The Sn atom is outside the C1PN plane. The Sn–N bond of **8** is longer than in Sn(II) amides {*cf.*, 2.09(1) Å in Sn[N(SiMe$_3$)$_2$]$_2$ [26a]} or eneamides {*cf.*, 2.130(3) Å in Sn[N(SiMe$_3$)C(Bu^t)=CH(C$_6$H$_3$Me$_2$-2,5)]$_2$ [15]}. Likewise, the Sn–C bond of **8** is long {*cf.*, 2.28 Å in Sn[CH(SiMe$_3$)$_2$]$_2$ [26b]}.

The reaction leading to the dimeric product [Sn(L^6)]$_2$ (**8**) was investigated using quantum chemical calculation techniques. Of the twelve isomers of complex **7**, two were considered further; of these, **7a** (Fig. 10), corresponds to that of the isoleptic lead compound (Pb(L^3)$_2$), [20]. It is noteworthy that the phenyl rings on adjacent phosphorus atoms, stack like the graphene layers in graphite, which is due to dispersive interactions. However, **7a** is not the energetically favoured isomer. Isomer **7b**, illustrated in Fig. 11, where the nitrogens are on the same side, has weaker Ph/Ph interaction. However, there is a clear interaction (see back view) from hydrogen (up right) to phenyl (down right). Isomer **7b** is favoured (MP2) over **7a** by 28.0 kJ/mol.

As with complex **5**, the energies for HL^3 and its dimer were calculated, with similar observations on the location of the hydrogen as between the monomer and the dimer. From the calculation on the dimerisation reaction it appears that the dimer is preferred at ⩽470 K, indicating that there is a significant difference to the related dimerisation of HL^2, (for which the temperature was ⩽210 K).

This may be due to dispersive interactions between the phenyl groups, as suggested by B3LYP calculations, which do not consider dispersion adequately.

Selected results of the final calculations for complex **5**, are shown in Fig. 12, together with the appropriate experimental X-ray data. Fig. 13 shows the MP2 calculated Gibbs free energies for the conversion **7a** or **7b** into **8** over a range of temperatures.

Front view   Back view

(ΔE = 28.0 kJ/mol).

C_2-symmetry

Sn–N: 2.481 Å

Sn–C (CH): 2.449 Å

N–Sn–N: 113.1°

C–Sn–C: 129.1°

Shortest C–C in Ph–Ph: 2.948 Å
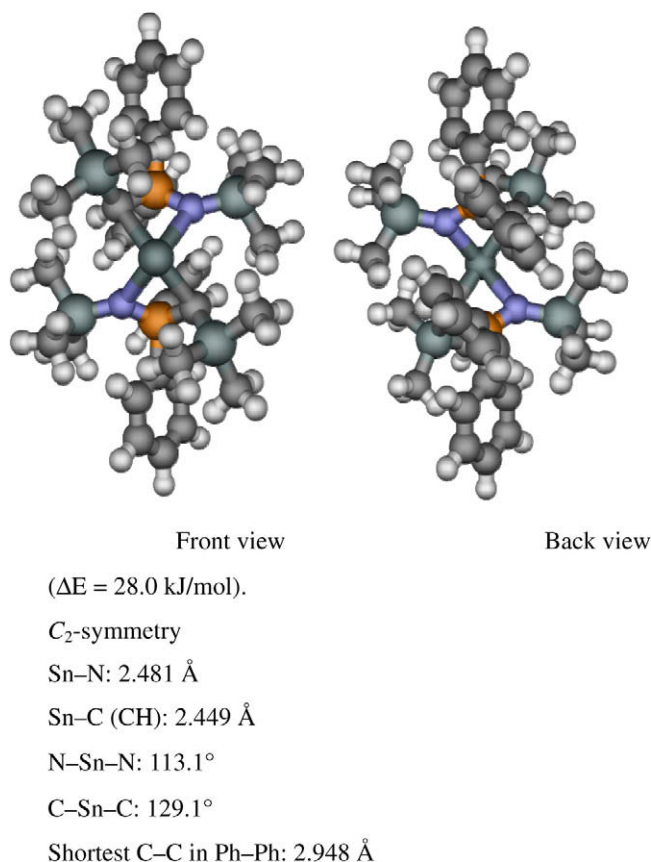
Fig. 10. MP2 calculated structure for **7a**, with selected geometrical parameters.
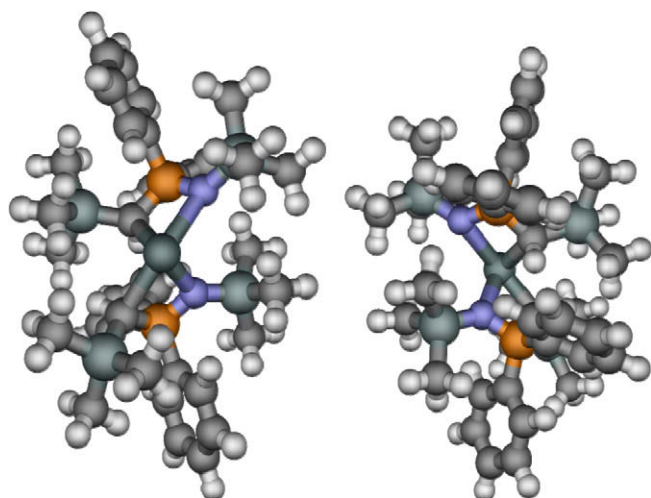
Front view   Back view

($\Delta E = 0.0$ kJ/mol).

C_1-symmetry

Sn–N: 2.697 Å; 2.307 Å

Sn–C (CH): 2.354 Å; 2.493 Å

N–Sn–N: 85.0°

C–Sn–C: 86.7°

H–C(Ph): 2.536 Å

Fig. 11. MP2 calculated structure for **7b,** with selected geometrical parameters.

8
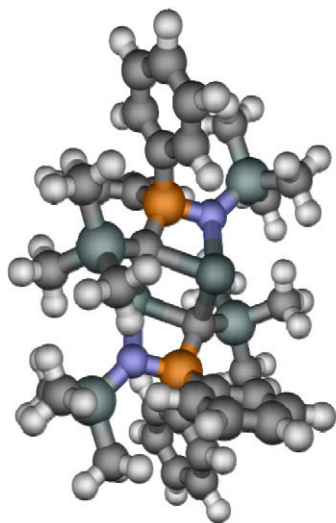
C_i-symmetry

Sn–N: 2.331 Å (2.308)

Sn–C1: 2.368 Å (2.313)

Sn–C1': 2.336 Å (2.313)

Sn–N–P: 92.9° (92.6)

Fig. 12. MP2 calculated structure for **5**, with selected calculated bond angles and lengths with crystal structure data in parentheses.
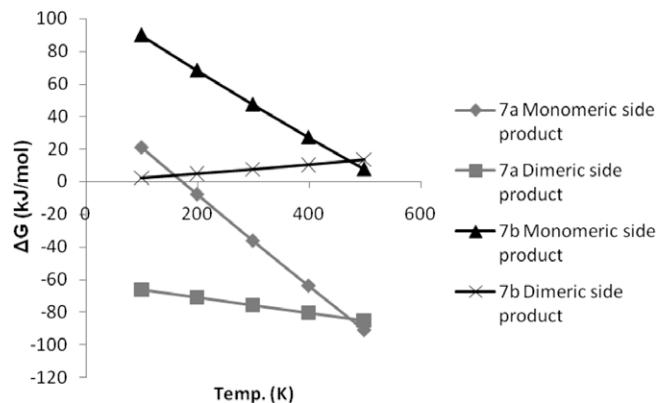
Fig. 13. MP2 calculated Gibbs free energy for reaction of **7a** or **7b** to **8** over a range of temperatures.

From these data it is concluded that **7a,** unlike **7b**, is unstable with respect to the reaction products **8** and HL^3.

The molecular structures of the crystalline $Sn(L^4)_2$ (**9**) (Fig. 14) and $Pb(L^4)_2$ (**10**) (Fig. 15) were determined by single crystal X-ray diffraction [24]. Selected geometric parameters are listed in Table 3 (**9**) and 4 (**10**). Each of **9** and **10** has the two L^4 ligands bound almost symmetrically about the pyramidal central M(II) atom, as illustrated for **10** in Fig. 16.

3. Conclusions

Reactions of (i) $SnBr_2$ with an equivalent portion of a 1-aza-allylpotassium compound $K(L^1)$ or $K(L^2)$ and (ii) $SnCl_2$ with an equivalent portion of the 1-aza-2-diphenylphospha(V)allyllithium compound $Li(L^3)$ are reported $[L^1 = CH(C_6H_3Me_2-2,5)C(Bu^t)-N-(SiMe_3);$ $L^2 = CH(Ph)C(Ph)N(SiMe_3);$ $L^3 = CH(SiMe_3)P(Ph)_2-N(SiMe_3)]$. Particularly noteworthy was the unexpected formation of the X-ray-characterised crystalline fused tricyclic compounds $[Sn(L^5)]_2$ (**5**) and $[Sn(L^6)]_2$ (**8**) from $2SnBr_2$ with $2 K(L^2)$ and $2SnCl_2$ with $2Li(L^3)$, respectively $[L^5 = C(Ph)C(Ph)N(SiMe_3);$ $L^6 = C(SiMe_3)P(Ph)_2N(SiMe_3)]$. The formation of **5** and **8** from their precursors has been modelled by quantum chemical calculations. Six new mononuclear tin(II) complexes containing the ligands L^1, L^2, L^3 or L^4 have been prepared and characterised (Table 4).

4. Experimental

4.1. General details

Syntheses were carried out under an atmosphere of argon or in a vacuum, using Schlenk apparatus and vacuum line techniques. The solvents used were reagent grade or better and were freshly distilled under dry nitrogen gas and freeze/thaw degassed prior to use. The drying agents employed were sodium benzophenone (C_6H_6, Et_2O, thf) or sodium-potassium alloy (C_5H_{12}, C_6H_{14}). The solvents for NMR spectroscopy (C_6D_6, C_5D_5N) were stored over molecular sieves (A4). Elemental analyses were obtained by Medac Ltd., Brunel University or The Metropolitan University, London. Melting points were measured in sealed capillaries. The ^1H, ^{13}C, ^{31}P and ^{119}Sn NMR spectra were recorded using a Bruker WM-360, DPX300 or AMX500 instrument and were referenced internally (^1H, ^{13}C) to residual solvent resonances or externally (^{31}P with 85% aq. H_3PO_4 as standard; ^{119}Sn with $SnMe_4$ as standard). Electron impact mass spectra were taken from solid samples, with a VG Autospec or a Kratos MS 80RF instrument. The compounds $H(L^3)$ [23], $[Li(L^3)(OEt_2)_2]$ [21], $[Li(L^3)]_2$ [21] $[L^3 = CH(SiMe_3)P(Ph)_2=NSiMe_3]$ were prepared by published procedures. Other chemical
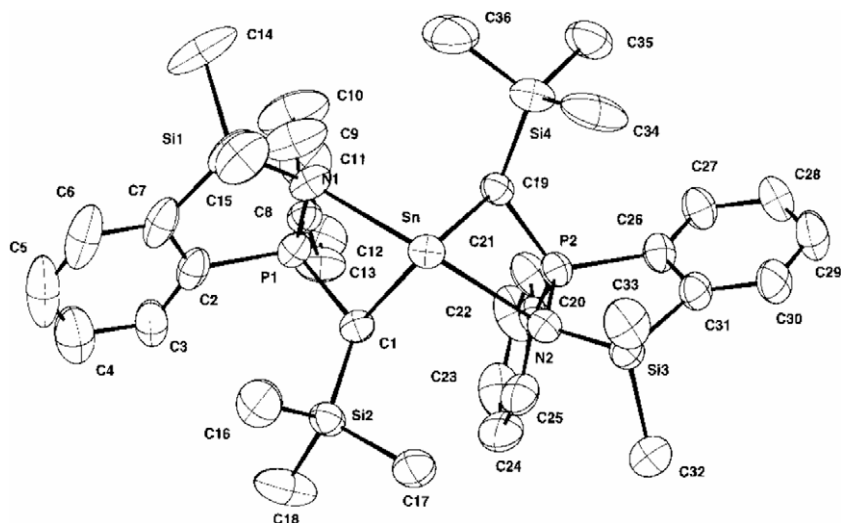
**Fig. 14.** ORTEP representation of the molecular structure of Sn(**L**⁴)₂ (**9**) [24].
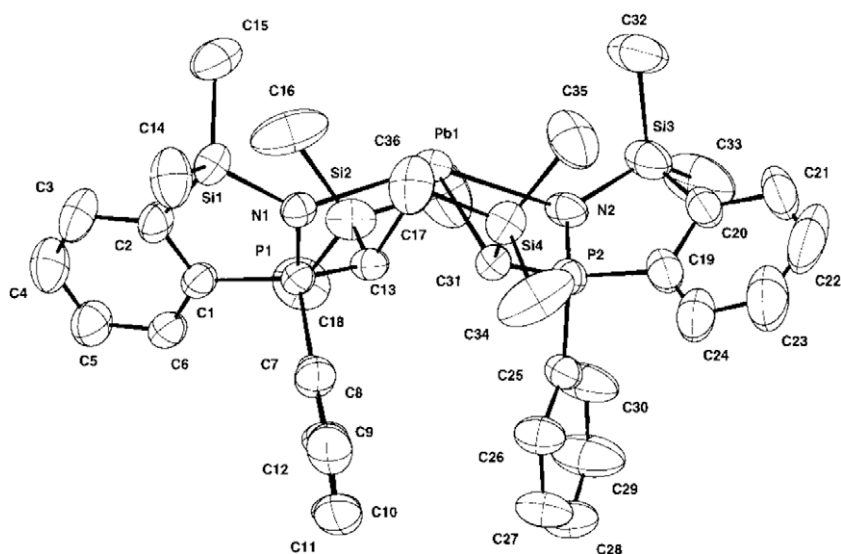
Fig. 15. ORTEP representation of the molecular structure of Pb(**L**⁺)₂ (**10**) [24].

Table 3
Selected bond distances (Å) and angles (°) for **9** [24].

Sn–C1	2.335(7)	Si1–N1	1.705(6)
Sn–C19	2.353(6)	Si3–N2	1.711(6)
Sn–N1	2.480(6)	P1–C2	1.813(8)
Sn–N2	2.525(6)	P2–C26	1.830(7)
P1–N1	1.599(6)	C2–C7	1.401(11)
P2–N2	1.592(6)	C26–C31	1.395(10)
P1–C1	1.751(7)	P2–C19	1.749(7)
C1–Sn–N1	68.4(2)	Sn–N1–P1	90.6(2)
C19–Sn–N2	67.5(2)	Sn–N2–P2	89.8(3)
N1–Sn–C19	89.3(2)	Sn–C1–P1	91.9(3)
N2–Sn–C1	88.8(2)	Sn–C19–P2	91.9(3)
N1–Sn–N2	146.7(2)	N1–P1–C1	107.9(3)
C1–Sn–C19	93.8(2)	N2–P2–C19	108.5(3)
C1–P1–C2	117.1(3)	N1–Si1–C7	97.9(4)
C19–P2–C26	117.6(3)	N2–Si3–C31	97.9(3)
P1–C2–C7	111.5(7)	P2–C26–C31	111.1(5)

Fig. 16. Schematic representation of **10**, showing the angular environment of the Pb atom [24].

4.2. Preparation of K[CH(C₆H₃Me₂-2,5)C(Buᵗ)NSiMe₃] [≡ K(**L**¹)]

A solution of 2,5-dimethylbenzyl chloride (25.0 g, 162 mmol) in diethyl ether (*ca.* 140 cm³) was slowly added to magnesium (4.50 g, 192 mmol) suspended in Et₂O (*ca.* 40 cm³). After *ca.* 12 h, chlorotrimethylsilane (18.4 g, 162 mmol) was added dropwise at ambient temperature. The mixture was stirred for *ca.* 12 h, whereafter water was added. The organic phase was separated and dried (CaCl₂). Distillation afforded 2,5-Me₂C₆H₃CH₂SiMe₃ (17.0 g, 53%), b.p. 46–56 °C/1 mmHg. LiBuⁿ in hexanes (25 cm³ of a 1.6 mol dm⁻³ solution in hexane) was slowly added to the above silane (7.80 g,

starting materials were purchased (Aldrich) and rigorously dried before use. Details of the X-ray diffraction data for [Sn(**L**⁶)]₂ (**8**), Sn(**L**⁴)₂ (**9**) and Pb(**L**⁴)₂ (**10**) are to be found in Ref. [24].

Table 4
Selected bond distances (Å) and angles (°) for **10** [24].

Pb–C13	2.450(7)	N1–Si1	1.706(6)
Pb–C31	2.429(7)	N2–Si3	1.691(6)
Pb–N1	2.607(5)	P1–C1	1.815(8)
Pb–N2	2.594(6)	P2–C19	1.817(11)
N1–P1	1.580(6)	C1–C2	1.395(10)
N2–P2	1.599(6)	C19–C20	1.449(13)
C13–P1	1.748(7)	C31–P2	1.762(6)
C13–Pb–N1	65.2(2)	Pb–N1–P1	90.4(2)
C31–Pb–N2	66.2(2)	Pb–N2–P2	90.5(2)
N1–Pb–C31	90.1(2)	Pb–C13–P1	92.0(3)
N2–Pb–C13	90.8(2)	Pb–C31–P2	92.4(3)
N1–Pb–N2	146.0(2)	N1–P1–C13	109.9(3)
C13–Pb–C31	92.7(2)	N2–P2–C31	109.5(3)
C13–P1–C1	117.1(4)	N1–Si1–C2	97.0(3)
C31–P2–C19	115.0(4)	N2–Si3–C20	95.6(4)
P1–C1–C2	111.0(6)	P2–C19–C20	107.7(9)

40 mmol) and tmeda (6.0 cm^3, 40 mmol) in light petroleum (b.p. 30–40 °C) at 0 °C. The mixture was stirred at ambient temperature for *ca.* 2 h, then Bu^{t}CN (4.4 cm^3, 40 mmol) was added with stirring which was continued for a further 2 h. Potassium *tert*-butoxide (4.9 g, 40 mmol) was added and the mixture set aside for *ca.* 12 h, then filtered. The precipitate of K(**L^1**) (11.5 g, 92%) was washed with light petroleum (2 × 40 cm^3) and dried *in vacuo*; ^{1}H NMR (C$_5$D$_5$N): δ 0.56 (s, 9 H), 1.48 (s, 9 H), 2.27 and 2.31 (s, 3 H), 5.48 (s, 1 H), 6.54 (m, 1 H), 7.15 (d, 2 H).

4.3. Preparation of K[CH(Ph)C(Ph)NSiMe$_3$] [$\equiv$ K(**L^2**)]

A hexanes solution of LiBu^n (73 cm^3 of a 1.6 mol dm^{-3} solution) was slowly added to benzyl(trimethyl)silane (19.0 g, 116 mmol) and tmeda (17 cm^3, 116 mmol) in light petroleum (b.p. 30–40 °C, *ca.* 60 cm^3) at ambient temperature. The mixture was stirred for 12 h, then filtered. The precipitate of Li{CH(SiMe$_3$)Ph}(tmeda) (27 g, 81%) was collected and dried. Benzonitrile (4.1 cm^3, 41 mmol) was added by syringe to this lithium compound (12.0 g, 42 mmol) in light petroleum (b.p. 60–80 °C, 40 cm^3) at ambient temperature. The mixture was stirred for 4 h, then KOBu^t (5.1 g, 42 mmol) was added. The mixture was stirred for a further 4 h. The precipitate was collected and washed with Et$_2$O (*ca.* 100 cm^3) and dried *in vacuo* to give the pale yellow K(**L^2**) (14.3 g, 94%). ^{1}H NMR (C$_5$D$_5$N): δ 0.24 (s, 9 H), 5.50 (s, 1 H), 6.81 (t, 1 H), 7.25 (m, 5 H), 7.72 (d, 2 H), 8.50 (d, 2 H).

4.4. Preparation of Sn[N(SiMe$_3$)C(Bu^t)C(H)C$_6$H$_3$Me$_2$-2,5]$_2$ {$\equiv$ [Sn(**L^1**)$_2$]} (**3**)

Tin(II) bromide (0.67 g, 2.50 mmol) was added to a stirred suspension of K(**L^1**) (1.50 g, 4.78 mmol) in Et$_2$O (*ca.* 50 cm^3) at ambient temperature for 16 h. The resulting yellow solution was filtered off from the white precipitate and solvent removed from the filtrate *in vacuo*. The bright yellow oily residue was then washed twice with light petroleum (b.p. 30–40 °C, *ca.* 20 cm^3) to give a pale yellow, free-flowing solid, which was dissolved in toluene (*ca.* 15 cm^3) and concentrated to *ca.* 5 cm^3. The solution in a Schlenk tube was then heated to *ca.* 80 °C, placed in a Dewar vessel filled with warm (*ca.* 60 °C) water and allowed to cool slowly. After 3 d, the water was removed and replaced by acetone. The Dewar vessel and Schlenk tube were cooled to −30 °C affording bright yellow crystals of complex **3** (1.23 g, 74%) (Anal. Calc. C$_{34}$H$_{56}$N$_2$Si$_2$Sn: C, 61.1; H, 8.40; N, 4.19. Found: C, 60.9; H, 8.45; N, 4.23%), mp 87 °C. ^{1}H NMR: δ 0.24 [s, 9 H, Si(CH$_3$)$_3$], 1.02 [s, 9 H, C(CH$_3$)$_3$], 1.91 (s, 3 H, C$_6$H$_3$CH$_3$-5), 2.15 (s, 3 H, C$_6$H$_3$CH$_3$-2), 5.09 (br s, 1 H, CH), 6.61–6.84 ppm [m, 3 H, C$_6$H$_3$(CH$_3$)$_2$]; ^{13}C NMR: δ 4.27 [q,

^{1}J(^{13}C–^{1}H) 118.5, Si(CH$_3$)$_3$], 20.27 [q, ^{1}J(^{13}C–^{1}H) 125.8, C$_6$H$_3$(CH$_3$)$_2$], 20.88 [q, ^{1}J(^{13}C–^{1}H) 125.8, C$_6$H$_3$(CH$_3$)$_2$], 30.6 [q, ^{1}J(^{13}C–^{1}H) 125.8, C(CH$_3$)$_3$], 41.84 [s, C(CH$_3$)$_3$], 104.4 [d, ^{1}J(^{13}C–^{1}H) 151.9 Hz, C(H)]; 132.4, 134.5, 138.5 (C$_6$-2,4,6), 151.1 ppm (CN); ^{29}Si{^{1}H} NMR: δ 0.27 ppm; ^{119}Sn{^{1}H} NMR: δ 61.5 ppm.

4.5. Preparation of [Sn{μ-C(Ph)C(Ph)NSiMe$_3$}]$_2$ {$\equiv$ [Sn(**L^5**)]$_2$} (**5**)

Tin(II) bromide (0.51 g, 1.8 mmol) was added to a stirred suspension of K(**L^2**) (1.13 g, 3.70 mmol) in Et$_2$O (*ca.* 50 cm^3) at ambient temperature and the mixture was set aside for 35 h with stirring. The mixture was filtered. The yellow filtrate was concentrated to *ca.* 20 cm^3 and stored at −30 °C. After 3 weeks, pale yellow crystals of **5** (0.36 g, 23%) (Anal. Calc. C$_{34}$H$_{38}$N$_2$Si$_2$Sn$_2$: C, 53.1; H, 4.95; N, 3.64. Found: C, 52.6; H, 4.90; N, 3.67%), mp < 120 °C (decomp.) were obtained. ^{1}H NMR (C$_5$D$_5$N): δ 0.21 [s, 9 H, Si(CH$_3$)$_3$], 5.71 (br s, 1 H, CH), 7.30 (m, 5 H, Ph), 7.75 ppm (m, 5 H, Ph). A small amount (*ca.* 50 mg) of [Me$_3$SiN=C(Ph)C(Ph)-]$_2$ was identified in the filtrate by ^{1}H NMR spectroscopy.

4.6. Preparation of Sn[CH(SiMe$_3$)P(Ph)=NSi(Me)$_2$C$_6$H$_4$-1,2]$_2$ {$\equiv$ [Sn(**L^4**)$_2$]} (**9**)

Tin(II) chloride (0.58 g, 3.05 mmol) was added to a solution of Li(**L^3**) (1.10 g, 3.01 mmol) in Et$_2$O (30 cm^3) at −78 °C with stirring. The mixture was allowed to warm at ambient temperature and was stirred overnight. The stirred mixture was recooled to −78 C and LiBu^n (1.9 cm^3 of a 1.6 mol dm^{-3} hexane solution, 3.04 mmol) was added dropwise. Stirring was continued for 4 h at room temperature. Solvent was removed *in vacuo* and the solid residue was extracted with hexane. The extract was filtered and the filtrate was concentrated to afford colourless crystals of **9** [0.65 g, 54% based on Li(**L^3**)] (Anal. Calc. C$_{36}$H$_{50}$N$_2$P$_2$Si$_4$Sn: C, 53.8; H, 6.27; N, 3.48. Found: C, 53.0; H, 6.18; N, 3.13%), mp 183–186 °C. ^{1}H NMR: δ 0.27 [s, 18 H, Si(CH$_3$)$_3$], 0.43 [s, 6 H, Si(CH$_3$)$_2$], 0.69 [s, 6 H, Si(CH$_3$)$_2$], 1.77 [d, 2 H, ^{2}J(^{1}H–^{31}P) 10.8 Hz]; 6.92–7.02 (m) and 7.39–7.49 (m) ppm (C$_6$H$_5$ and C$_6$H$_4$); ^{13}C{^{1}H} NMR: δ 0.74 [d, J(^{13}C–^{31}P) 6.2, SiCH$_3$], 1.60 [d, J(^{13}C–^{31}P) 3.8, SiCH$_3$], 2.63 [d, J(^{13}C–^{31}P) 2.1, SiCH$_3$], 18.94 [d, ^{2}J(^{13}C–^{31}P) 54.7, CH], 127.5 [d, J(^{13}C–^{31}P) 13.5], 128.5 [d, J(^{13}C–^{31}P) 10.0], 128.7 [d, J(^{13}C–^{31}P) 11.5], 129.1 [d, J(^{13}C–^{31}P) 10.5], 129.8 [d, J(^{13}C–^{31}P) 2.6], 129.9 [d, J(^{13}C–^{31}P) 2.5], 131.6 [d, J(^{13}C–^{31}P) 16.5], 140.5 [d, ^{1}J(^{13}C–^{31}P) 85.7], 148.3 [d, ^{1}J(^{13}C–^{31}P) 75.3], 149.7 ppm [d, J(^{13}C–^{31}P) 30.2 Hz]; ^{29}Si{^{1}H} NMR: δ −0.42 [s, with satellites, ^{2}J(^{29}Si–$^{119/117}$Sn) 53.5], 8.53 ppm [d, ^{2}J(^{29}Si–^{31}P) 7.3 Hz]; ^{31}P{^{1}H} NMR: δ 44.9 ppm [s, with satellites, ^{2}J(^{31}P–$^{119/117}$Sn) 155.5, 162.3 Hz]; ^{119}Sn{^{1}H} NMR: δ 121.4 ppm [t, ^{2}J(^{119}Sn–^{31}P) 162.5 Hz].

4.7. Preparation of [Sn{μ-C(SiMe$_3$)P(Ph)$_2$NSiMe$_3$}]$_2$ {$\equiv$ [Sn(**L^6**)]$_2$} (**8**) and Sn(**L^3**)$_2$ (**7**)

n-Butyllithium (2.25 cm^3 of a 1.6 mol dm^{-3} hexane solution, 3.52 mmol) was added dropwise to a solution of H(**L^3**) (1.22 g, 3.40 mmol) in Et$_2$O (30 cm^3) at −20 °C, brought to ambient temperature and set aside for 3 h. Tin(II) chloride (0.32 g, 1.68 mmol) was added to the Li(**L^3**) solution at −40 °C. The mixture was stirred at ambient temperature for 12 h. Volatiles were removed *in vacuo* and the residue was extracted with pentane (20 cm^3). The extract was concentrated to *ca.* 5 cm^3, which after 12 h afford the yellow crystalline complex **8** (0.77 g, 96%). (Anal. Calc. C$_{38}$H$_{56}$N$_2$P$_2$Si$_4$Sn$_2$: C, 47.9; H, 5.92; N, 2.94. Found: C, 48.0; H, 5.94; N, 2.87%), mp 216–219 °C. Complex **8** was sparingly soluble in pentane or hexane but soluble in benzene or diethyl ether. It was stable for only about 3 weeks in the solid state or 4 d in benzene at ambient temperature. The NMR spectra of a freshly prepared sample in C$_6$D$_6$ were consistent with it being Sn(**L^3**)$_2$ (**7**); for selected ^{13}C, ^{31}P, ^{119}Sn NMR spectral data, see Table 2. ^{1}H NMR: δ 0.04 [s, 18 H, NSi(CH$_3$)$_3$],

Table 5
Mass spectral data (EI–70 eV) for **3**, **5**, **6**, **8**, **9**[a] and **10**.[a]

Compound		*m/e* (relative intensity, %), and assignment
$Sn(L^1)_2$	(**3**)	667 (100), $[M]^+$; 652 (63), $[M - Me]^+$; 594 (74), $[M - SiMe_3]^+$; 421 (65), $[M - L^1]^+$
$[Sn\{\mu\text{-}C(Ph)C(Ph)NSiMe_3\}]_2$	(**5**)	767 (21), $[M + 1]^+$; 695 (54), $[M + 1 - SiMe_3]^+$; 622 (44), $[M + 1 - 2SiMe_3]^+$; 174 (63), $[Ph_2C_2]^+$
$Sn(L^3)Cl$	(**6**)	513 (21), $[M]^+$; 478 (8), $[M - Cl]^+$; 422 (2), $[M - Cl - SiMeCH]^+$; 359 (50), $[L^3]^+$
$[Sn\{\mu\text{-}C(SiMe_3)P(Ph)_2NSiMe_3\}]_2$	(**8**)	730 (1), $[M + 1 - 2SiMe_3 - Ph]^+$; 641 (2), $[M + 1 - 2SiMe_3 - 2Ph]^+$; 567 (6), $[M + 1 - 3SiMe_3 - 2Ph - N]^+$; 552(3), $[M + 1 - 3SiMe_3 - 2Ph - N - Me]^+$
$Sn[CH(SiMe_3)P(Ph)(1,2\text{-}C_6H_4)=NSiMe_2]_2$	(**9**)	920 (38), $[2M - L^3]^+$; 848 (4), $[2M - L^3 - SiMe_3]^+$; 804 (1), $[M]^+$; 578 (10), $[M - Ph - C_6H_4 - SiMe_3]^+$
$Pb[CH(SiMe_3)P(Ph)(1,2\text{-}C_6H_4)=NSiMe_2]_2$	(**10**)	892 (5), $[M]^+$; 550 (70), $[M - L^4]^+$; 472 (20), $[M - L^4 - C_6H_4]^+$; 342 (100), $[L^4]^+$

[a] $[M]^+$ represents the parent molecular ion; only the four highest *m/e* peaks are listed.

0.29 [s, 18 H, CSi(CH₃)₃], 1.71 [d, 2 H, $^1J(^1H\text{-}^{31}P)$ 15.7 Hz, CH (confirmed by a DEPT experiment)], 6.95–6.98 (m), 7.15–7.10 (m), 7.57–7.63 (m), 7.79–7.84 ppm (m) (C₆H₅); $^{13}C\{^1H\}$ NMR: δ 2.82 [d, $J(^{13}C\text{-}^{31}P)$ 4.5, Si(CH₃)₃], 4.15 [d, $J(^{13}C\text{-}^{31}P)$ 3.2, SiCH₃], 24.76 [d, $J(^{13}C\text{-}^{31}P)$ 62.8, CH]; 128.1 (s), 130.8 (d), 131.5 [d, $J(^{13}C\text{-}^{31}P)$ 10.6], 132.0 [d, $J(^{13}C\text{-}^{31}P)$ 10.5], 139.1 [d, $J(^{13}C\text{-}^{31}P)$ 80.6], 139.2 ppm [d, $J(^{13}C\text{-}^{31}P)$ 85.7 Hz] (Ph); $^{31}P\{^1H\}$ NMR: δ 25.45 ppm [s, with satellite peaks at $^2J(^{31}P\text{-}^{119/117}Sn)$ 160.5, 167.1 Hz]; $^{119}Sn\{^1H\}$ NMR: δ 82.3 ppm [t, $^2J(^{119}Sn\text{-}^{31}P)$ 167.6 Hz].

4.8. Preparation of mixtures with H(L³) of Sn[CH(SiMe₃)P(Ph)₂NSiMe₃]₂ (**7**) and [Sn(L⁶)]₂ (**8**)

Solid tin(II) chloride (0.17 g, 0.897 mmol) was added to a stirred solution of Li(L³) (0.68 g, 1.86 mmol) in hexane (40 cm³) at −40 °C, to which Et₂O (40 cm³) was added. The mixture was stirred for 21 h at ambient temperature, then filtered. Volatiles were removed from the filtrate *in vacuo* yielding a mixture of **7** and H(L³) as a sticky solid. The NMR data (integration of Ph signals excluded) were as follows: ^1H NMR: δ 0.04 (s, 18 H, CSiMe₃), 0.22 (s, 18 H, NSiMe₃), 1.71 [d, 2 H, $^1J(^1H\text{-}^{31}P)$ 15.7 Hz], 6.94–7.81 ppm (m, Ph); $^{31}P\{^1H\}$ NMR: δ 25.45 ppm [s, with satellites $^2J(^{31}P\text{-}^{119}Sn)$ 167 Hz]; $^{119}Sn\{^1H\}$ NMR: δ 82.3 ppm [t, $^2J(^{119}Sn\text{-}^{31}P)$ 167 Hz].

A solution of **7** in C₆D₆ was stored in an NMR tube for 28 d, when all traces of signals of **7** had disappeared and the following data (attributed to **8**) were recorded: ^1H NMR: δ −0.25 (s, 9 H, CSiMe₃), 0.15 (s, 9 H, NSiMe₃), 6.81–7.72 ppm (m, Ph); $^{31}P\{^1H\}$ NMR: δ 27.77 ppm [s, with satellites $^2J(^{31}P\text{-}^{119}Sn)$ 138 Hz]; $^{119}Sn\{^1H\}$ NMR: δ 530.3 ppm [t, $^2J(^{119}Sn\text{-}^{31}P)$ 147 Hz].

4.9. Preparation of Pb[CH(SiMe₃)P(Ph)(1,2-C₆H₄)=NSiMe₂]₂ {≡ [Pb(L⁴)₂} (**10**)

From lead(II) chloride (0.23 g, 0.82 mmol) and a solution of Li(L⁴) (0.57 g, 1.63 mmol) in Et₂O (20 cm³), using a procedure similar to that for Sn(L⁴)₂ (Section 4.6), there were obtained colourless crystals of **10** (0.35 g, 48%) (Anal. Calc. C₃₆H₅₀N₂P₂Si₄Pb: C, 48.5; H, 5.65; N, 3.14. Found: C, 47.9; H, 5.65; N, 3.09%), mp 90–92 °C. ^1H NMR: δ 0.31 [s, 18 H, Si(CH₃)₃], 0.53 [s, 6 H, Si(CH₃)₂], 0.69 [s, 6 H, Si(CH₃)₂], 1.43 [d, 2 H, $^2J(^1H\text{-}^{31}P)$ 9.5 Hz]; 7.06–7.25 (m) and 7.54–7.65 ppm (m, Ph, C₆H₄); $^{13}C\{^1H\}$ NMR: δ 1.63 [d, $J(^{13}C\text{-}^{31}P)$ 6.2, SiCH₃], 2.01 [d, $J(^{13}C\text{-}^{31}P)$ 3.9, SiCH₃], 2.39 [d, $J(^{13}C\text{-}^{31}P)$ 2.41, SiCH₃], 28.2 [d, $^2J(^{13}C\text{-}^{31}P)$ 61.9, CH]; 127.0 [d, $J(^{13}C\text{-}^{31}P)$ 13.4], 128.5 [d, $J(^{13}C\text{-}^{31}P)$ 11.2], 129.1 [d, $J(^{13}C\text{-}^{31}P)$ 10.2], 129.7 [d, $J(^{13}C\text{-}^{31}P)$ 2.8], 129.9 [d, $J(^{13}C\text{-}^{31}P)$ 2.8], 131.1 [d, $J(^{13}C\text{-}^{31}P)$ 16.5], 141.3 [d, $^1J(^{13}C\text{-}^{31}P)$ 86.9], 148.0 [d, $^1J(^{13}C\text{-}^{31}P)$ 30.8], 153.6 ppm [d, $J(^{13}C\text{-}^{31}P)$ 77.0 Hz]; $^{31}P\{^1H\}$ NMR: δ 40.3 ppm [s, with satellites, $J(^{31}P\text{-}^{119}Sn)$ 311.8 Hz]; $^{207}Pb\{^1H\}$ NMR: δ 1998.3 ppm [t, $^2J(^{207}Pb\text{-}^{31}P)$ 313.3 Hz].

4.10. Mass spectra of **3**, **5**, **6**, **8**, **9** and **10**

The four highest *m/e* peaks of the EI-mass spectrum for each of compounds **3**, **5**, **6**, **8**, **9** and **10** with assignments are listed in Table 5.

4.11. X-ray crystallographic study of **5**

Diffraction data were collected at 293(2) K on an Enraf-Nonius CAD 4 diffractometer using monochromated Mo Kα radiation (λ = 0.71069 Å). Crystals were mounted under an inert atmosphere into a capillary which was then sealed. The structure was refined on all F^2 using SHELXL-97 [27]. Further details are in Table 6. There are two independent molecules in the unit cell of essentially the same geometry.

4.12. Quantum chemical calculations

All molecules were fully optimised by the MP2 method, utilising the resolution of the identity (RI) technique [28] as implemented in the TURBOMOLE version 5.10 [29]. A triple-zeta valence basis set (def-TZVP) [30,31], together with the corresponding RI auxiliary basis set [32], was applied for all atoms, and for tin a 46 electron relativistic effective core potential (ECP) was used [33]. Symmetry constraints were employed when applicable. Each structure was verified as a true minimum in the potential energy surface by performing vibrational frequency calculations, also required for obtaining the Gibbs free energies.

Table 6
Crystal and refinement for **5**.

Formula	$C_{34}H_{38}N_2Si_2Sn_2$
M	768.22
Crystal system	Triclinic
Space group	$P\bar{1}$(No. 2)
a (Å)	12.369(3)
b (Å)	12.501(5)
c (Å)	13.058(4)
α (°)	99.19(3)
β (°)	116.55(3)
γ (°)	101.37(3)
V (Å³)	1698.5(9)
Z	2
Absorption coefficient (mm⁻¹)	1.57
Unique reflections,	5964
Reflections with $I > 2\sigma(I)$	3962
Final R indices [$I > 2\sigma(I)$]	R_1 0.051, wR_2 0.085
R indices (all data)	R_1 0.095, wR_2 0.100

Acknowledgements

Appendix A. Supplementary data

CCDC 730721 contains the supplementary crystallographic data for this paper. These data can be obtained free of charge from The Cambridge Crystallographic Data Centre via www.ccdc.cam.ac.uk/data_request/cif. Supplementary data associated with this article can be found, in the online version, at doi:10.1016/j.jorganchem.2009.06.025.

References

[1] J. Satgé, M. Massol, P. Rivieŕe, J. Organomet. Chem. 56 (1973) 1.
[2] W.P. Neumann, A. Schwarz, Angew. Chem., Int. Ed. Engl. 14 (1975) 812.
[3] J.W. Connolly, Adv. Organomet. Chem. 19 (1981) 123.
[4] W.P. Neumann, in: M. Gielen, P.G. Harrison (Eds.), The Organometallic and Coordination Chemistry of Germanium, Tin and Lead, Freund, Tel Aviv, 1978, p. 51.
[5] M.F. Lappert, Main Group Metal Chem. 17 (1994) 183.
[6] J.T.B.H. Jastrzebski, G. van Koten, Adv. Organomet. Chem. 35 (1993) 241.
[7] L. Bourget-Merle, M.F. Lappert, J.R. Severn, Chem. Rev. 102 (2002) 3031.
[8] N. Nimitsiriwat, V.C. Gibson, E.L. Marshall, A.J.P. White, S.H. Dale, M.R.J. Elsegood, Dalton Trans. (2007) 4464.
[9] F.T. Edelmann, Adv. Organomet. Chem. 57 (2008) 183.
[10] C.F. Caro, M.F. Lappert, P.G. Merle, Coord. Chem. Rev. 219–221 (2001) 605.
[11] W.-P. Leung, Z.-X. Wang, H.-W. Li, T.C.W. Mak, Angew. Chem., Int. Ed. 40 (2001) 2501.
[12] (a) W.-P. Leung, Z.-W. Wang, H.W. Li, Q.-C. Yang, T.C.W. Mak, J. Am. Chem. Soc. 123 (2001) 8123;
    (b) W.-P. Leung, K.-W. Wong, Z.-X. Wang, T.C.W. Mak, Organometallics 25 (2006) 2037.
[13] B.S. Jolly, M.F. Lappert, L.M. Engelhardt, A.H. White, C.L. Raston, J. Chem. Soc., Dalton Trans. (1993) 2653.
[14] W.-P. Leung, W.-H. Kwok, L.-H. Weng, L.T.C. Law, Z.-Y. Zhou, T.C.W. Mak, J. Chem. Soc., Dalton Trans. (1997) 4301.
[15] P.B. Hitchcock, J. Hu, M.F. Lappert, M. Layh, J.R. Severn, J. Chem. Soc., Chem. Commun. (1997) 1189.
[16] P.B. Hitchcock, M.F. Lappert, M. Layh, Inorg. Chim. Acta 269 (1998) 181.
[17] P.B. Hitchcock, M.F. Lappert, M. Layh, D.-S. Liu, R. Sablong, S. Tian, J. Chem. Soc., Dalton Trans. (2000) 2301.
[18] L. Brandsma, H.D. Verkruijsse, Preparative Polar Organometallic Chemistry, vol. 1, Springer Verlag, Berlin, Heidelberg, 1987.
[19] (a) H. Preut, H.-J. Haupt, F. Huber, Z. Anorg. Allg. Chem. 396 (1973) 81;
    (b) V.K. Belsky, N.N. Zemlyansky, N.D. Kolosova, I.V. Borisova, J. Organomet. Chem. 215 (1981) 41;
    (c) S. Masamune, L.R. Sita, J. Am. Chem. Soc. 105 (1983) 630;
    (d) S. Adams, M. Dräger, J. Organomet. Chem. 288 (1985) 295;
    (e) L.R. Sita, I. Kinoshita, J. Am. Chem. Soc. 111 (1989) 6454.
[20] P.B. Hitchcock, M.F. Lappert, Z.-X. Wang, J. Chem. Soc., Chem. Commun. (1997) 1113.
[21] P.B. Hitchcock, M.F. Lappert, P.G.H. Uiterweerd, Z.-X. Wang, J. Chem. Soc., Dalton Trans. (1999) 3413.
[22] B. Wrackmeyer, C. Stader, K. Horchler, J. Magn. Reson. 83 (1989) 601.
[23] P.B. Hitchcock, M.F. Lappert, Z.-X. Wang, J. Chem. Soc., Dalton Trans. (1997) 1953.
[24] Z.-X. Wang, D. Phil. Thesis, University of Sussex, 1996.
[25] M. Veith, V. Huch, J. Organomet. Chem. 308 (1986) 263.
[26] (a) T. Fjeldberg, H. Hope, M.F. Lappert, P.P. Power, A.J. Thorne, J. Chem. Soc., Chem. Commun. (1983) 639;;
    (b) D.E. Goldberg, P.B. Hitchcock, M.F. Lappert, K.M. Thomas, A.J. Thorne, T. Fjeldberg, A. Haaland, B.E.R. Schilling, J. Chem. Soc., Dalton Trans. (1986) 2387.
[27] G. M. Sheldrick, SHELXL-97, University of Göttingen, Göttingen, Germany, 1997.
[28] F. Weigend, M. Häser, Theor. Chem. Acc. 97 (1997) 331.
[29] R. Ahlrichs, M. Bär, M. Häser, H. Horn, C. Kölmel, Chem. Phys. Lett. 162 (1989) 165.
[30] A. Schäfer, C. Huber, R.J. Ahlrichs, Chem. Phys. 100 (1994) 5829.
[31] K. Eichkorn, F. Weigend, O. Treutler, R. Ahlrichs, Theor. Chem. Acc. 97 (1997) 119.
[32] F. Weigend, M. Häser, H. Patzelt, R. Ahlrichs, Chem. Phys. Lett. 294 (1998) 143.
[33] A. Bergner, M. Dolg, W. Kuechle, H. Stoll, H. Preuss, Mol. Phys. 80 (1993) 1431.